Scalable Computing: Practice and Experience, ISSN 1895-1767, http://www.scpe.org
© 2024 SCPE. Volume 25, Issues 5, pp. 3355–3365, DOI 10.12694/scpe.v25i5.3089

PROCESS TESTING AND ALGORITHM DETECTION ANALYSIS OF MECHANICAL STRENGTH OF ELECTROMECHANICAL COUPLING IN THE MAIN DRIVE OF ROLLING MILL

DONGBAO ZENG* AND HAI YAO†

Abstract. In order to deeply analyze the compressive strength of the electromechanical coupling system of the main drive of the rolling mill, this work takes the electromechanical coupling system of the main drive of the R2 rolling mill as a subject to study and analyze. First, experiments are designed to test the strength and some mechanical parameters of the main drive electromechanical coupling system of the R2 rolling mill, including the introduction of the main drive system of the R2 reversible rolling mill, test content, test scheme, test system framework and test materials. Next, this work analyzes the strength of the main drive shaft in the electromechanical coupling system of the main drive of the R2 rolling mill, and theoretically checks the fatigue strength of the main drive shaft, including the static strength analysis of the main drive shaft. Finally, this work analyzes the experimental data. The research shows that: (1) the peak value of the lower torque of the main drive coupling electromechanical of the R2 rolling mill is mainly distributed in the range of 650∼1550 mk N. The average value of the upper torque is mainly distributed in the range of 350∼1100 mk N. (2) The peak value of principal stress at $1^{\#}$ measuring point is within the range of 10-35Mpa, and the mean value of principal stress is within the range of -24-24Mpa. The peak value of principal stress at the $2^{\#}$ measuring point is in the range of 5-25Mpa, and the mean value of principal stress is in the range of -16-16Mpa. (3) When the upper drive shaft of the rolling mill runs at a working angle of 1.02°, the maximum Von Mises Stress of the drive shaft of the rolling mill is 95.10MPa. When the drive shaft of the rolling mill operates at a working angle of 3.14°, the maximum Von Mises Stress of the drive shaft of the rolling mill is 95.15MPa. This work aims to provide a theoretical reference for enhancing the compressive strength of the electromechanical coupling system of the main drive of the rolling mill.

Key words: electromechanical coupling system of the main drive of the rolling mill, compressive strength, main drive shaft, principal stress, fatigue strength

1. Introduction. The main characteristics of modern rolling mills are large, heavy load, high speed, continuous automation, precision and poor working conditions. These characteristics require the long service life of the main parts of the rolling mill. In order to achieve this goal, it is the most effective and convenient means to use modern mechanical methods and fully use the idea of the finite element method (FEM) and its generated software to study classical mechanical problems. Meanwhile, it is essential to apply advanced test technology for equipment diagnosis to provide conditions for analyzing the mechanical behavior of equipment [1]. In the past decade, the rapid development of computer hardware technology and the rapid decline of computer costs have greatly driven the development of finite element calculation software, and the function of display programs has also been increasingly enhanced. It provides a broad platform for the use of FEM to solve practical engineering problems [2]. Besides, as early as the 1960s, foreign steel companies noticed the impact of torsional vibration on the main drive system of the rolling mill, and have conducted massive experimental studies. At that time, the research level was limited to experimental measurement and the establishment of simple mechanical models, and there was no more in-depth theoretical exploration [3]. For example, in the 1960s, the Bethlehem Steel Corp of the United States conducted field tests and theoretical analysis on the rolling mill, and analyzed the resonance problem caused by the coupling of the frequency of the rolling mill drive system and the natural vibration frequency of the motor riser [4]. In 1973, the Association of Iron & Steel Engineers in America and Jones&Lauhlin Iron and Steel Company studied the torsional vibration of a rolling mill. They reached the following conclusions: the head of the hot top is conducive to reducing part of the mechanical coefficient; it is important to eliminate the clearance in the transmission link to reduce the value; shear parts should not be used as mechanical insurance parts [5].

*Jiangxi Technical College of Manufacturing, Nanchang, Jiangxi, 330095, China (DongbaoZeng2@163.com)
†Mechanical College, Shanghai Dianji University, Shanghai, 201306, China. (Corresponding author, HaiYao17@126.com)

Table 2.1: Main technical parameters of R2 reversible rolling mill

Parameter name	Specific value
Working roll diameter	1200/1100 mm
Support roll diameter	1600/1440 mm
Roller length	2250 mm
Rolling force	45000 kN
Motor power	2×7500 KW
Motor speed	0∼45/100 rpm
Balance coefficient of balance cylinder	1.1 (test condition), 1.3 (damage condition)

It was not until the 1970s that the torsional vibration of the rolling mill was paid attention to in China. In particular, several serious equipment accidents related to system torsional vibration have occurred in several domestic steel rolling plants in the past decade, which has caused people to study the impact of torsional vibration load on the system [6]. For example, the University of Science and Technology Beijing has studied the main drive system of the blooming mill of Baotou Iron and Steel Company and the second blooming mill of Anshan Iron and Steel Company. It is found that the self-excited vibration caused by roll slipping is the main cause of the main drive torsional vibration damage [7]. Professors at the University of Science and Technology Beijing adopted the rolling mill's shafting parameter optimization design method to predict and reduce the torque amplification factor in the design [8]. Wuhan University of Science and Technology studied the vibration of the arc joint shaft of the 1700 cold chain mill drive system of Wuhan Iron and Steel Company. It is found that the rolling speed greatly impacts the vibration of the shaft. The misalignment of the arc joint shaft causes polarization and gearbox meshing excitation [9].

In the rolling system, due to the manufacturing process, assembly and other factors, there is often a certain gap at the system's connection, which will make the stiffness of the main transmission system behave as nonlinear. Hence, the system cannot be simply described by a linear model. Avoiding the resonance synchronization phenomenon in the working process of the system, the reasonable control of the main drive system of the rolling mill, the establishment of the vibration simulation mechanical model and the torsional vibration of the system in case of slipping. Based on the above contents, for the frequent fracture accidents and fatigue damage of the main drive system of the rolling mill, this work takes the R2 four-roll reversing roughing mill of a certain unit as the research object. Then, based on the field test, combined with the worldwide torsional vibration research of the main drive system of the rolling mill, the dynamic characteristics analysis of the main drive system of the R2 rolling mill is conducted. Moreover, the FEM analysis software ANSYS is adopted to carry out three-dimensional (3D) FEM analysis on the spider universal joint of the main drive system of the R2 rolling mill. Moreover, the strength and fatigue check of the drive shaft in the main drive system of the R2 rolling mill are analyzed in detail. This work aims to design relevant simulation experiments to study the vibration of a rolling mill and analyze its strength to make a beneficial combination and supplement between theory and practice. It has crucial engineering practical significance and theoretical research significance.

2. Design of process test and simulation model.

2.1. Parameters test of mechanical mechanics in main drive electromechanical coupling system of R2 rolling mill .

(1) Main drive system of R2 reversible rolling mill.

1. Schematic diagram of the main drive system of the R2 reversing rolling mill
   The main drive system of the R2 reversible rolling mill adopts two synchronous motors to directly drive the upper and lower rolls. Figure 2.1 is the structure diagram.
2. Main technical parameters of R2 reversible rolling mill
   Table 2.1 displays the main technical parameters of the R2 reversible rolling mill.

(2) Field test content. The test content of this experiment mainly includes the torque M1 and M2 of the upper and lower drive shafts of the R2 reversible rolling mill, the stress $\sigma$of the lower connecting shaft, and rolling force P.

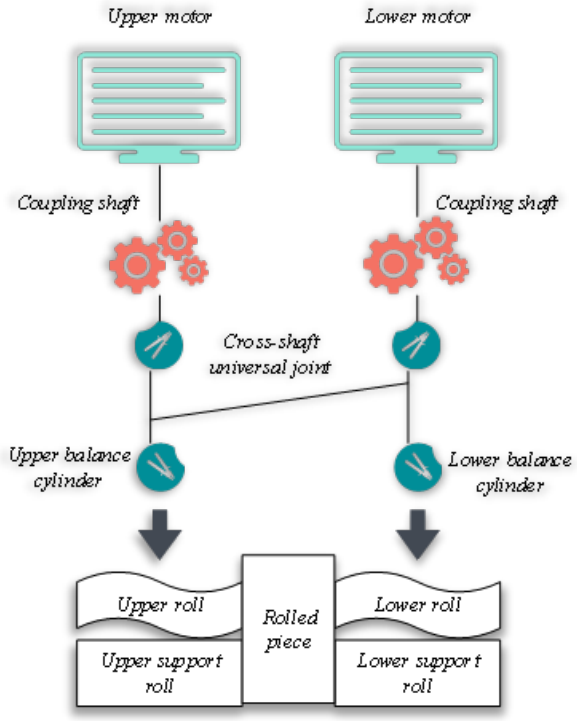

Fig. 2.1: Structural diagram of the main drive system of the R2 rolling reversible mill

(3) Test plan.

1. Measuring point position and testing method of main drive torque of R2 rolling mill:
   The test positions of the upper drive shaft torque and the lower drive shaft torque are as follows. The measuring point is located at the hollow shaft section with an outer diameter of D=930mm and an inner diameter of d=736mm. On this shaft section, four resistance pieces are pasted in the direction of ±450 with the axis to form a full-bridge test circuit. The signal is input into the YD-28A dynamic strain gauge through the slip ring, and then recorded by the computer after A/D conversion. The calibration is carried out with a constant-strength graduated beam. Resistance strain gauges, R1+R3 and R2+R4, are respectively attached to the constant strength beam's upper (tension) and lower (compression) sides, forming a full-bridge test circuit. Then, it is calibrated with standard weight loading. The torque calibration value of the upper drive shaft is K=24.237MPa/V, and the torque calibration value of the lower drive shaft is K=24.190MPa/V.
2. R2 rolling force:
   After the rolling force P of the R2 rolling mill is isolated through the isolator, it is led from the main electrical room to the test site through the shielded cable and connected to the computer. The calibration value of the rolling force is 450t/V (provided by a two-roll hot-rolling electrical workshop).
3. Location and test method of main drive stress measuring point of R2 rolling mill:
   The stress is measured through resistance strain. Because the stress situation of the shaft is complex and the direction of the principal stress is unknown, the strain rosette is adopted to measure the stress at this point. The distance between the main drive shaft $1^{\#}$ stress measuring point and the center line of the main shaft arm is 793 mm. The signals corresponding to the strain gauges in the horizontal direction (0°), 45° and vertical direction (90°) are $3^{\#}$, $4^{\#}$ and $5^{\#}$, respectively. The distance between the main drive shaft $2^{\#}$ stress measuring point and the center line of the main shaft arm is 643mm. The

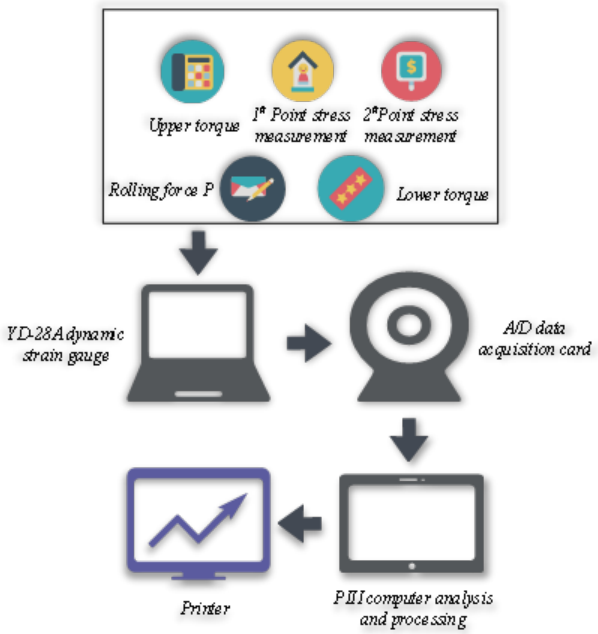

Fig. 2.2: Test system framework

signals corresponding to the strain gauges in the horizontal direction (0°), 45° and vertical direction (90°) are $2^{\#}$, $7^{\#}$ and $6^{\#}$, respectively. Considering that the temperature of the measuring point will change during the rolling process, in order to compensate for the test error caused by the temperature change, a small steel block (without stress) is placed near the measuring point as the temperature compensation block (the same as the temperature of the measuring point). Three resistance strain gauges are pasted on each temperature compensation block, and a half-bridge test circuit is formed with the three working pieces of the strain rosette at the measuring point.

The calibration is conducted with a constant-strength graduated beam. On the constant-strength graduated beam, a resistance strain gauge R1 is pasted and a temperature compensation block is placed near the measuring point. The resistance strain gauge R2 is attached on the temperature compensation block, and R1 and R2 form a half-bridge test circuit. The stress calibration value of each measuring point can be obtained by using standard weight loading for calibration. The calibration value of $3^{\#}$ is K=97.087MPa/V, that of $4^{\#}$ is K=97.276MPa/V, that of $5^{\#}$ is K=96.712MPa/V, that of $2^{\#}$ is K=96.900MPa/V, that of $7^{\#}$ is K=97.466MPa/V, and that of $6^{\#}$ is K=97.087MPa/V.

(4) Test system block diagram. The stress signal of each measuring point is connected to the dynamic strain gauge and recorded by the computer after A/D conversion. The sampling frequency of each channel is 100Hz. Figure 2.2 displays the system test block diagram.

(5) Test materials. The force and energy parameters of the main drive system during the rolling process of 174 steel billets of 11 rolling varieties produced by a certain unit were tested. Table 2.2 shows the specification and quantity of the test billet.

2.2. Research on strength and fatigue strength check of the main drive shaft of the R2 rolling mill.

(1) Mechanical analysis of the main drive shaft of the rolling mill.

1. FEM software

With the continuous progress of computer technology, the theoretical technology of Computer Aided Engineering (CAE) is also maturing [10]. Many kinds of FEM software can be used in the project,

Table 2.2: Specification and quantity of test billet

Material and model	Product specification (thick × wide × Length) (mm)	Slab quantity (block)
DC01	250×1300×8600	2
Q235A	230×1550×8600	2
RCL380	230×1550×8000	5
Q235A	230×1550×10800	3
St52-3	230×1700×10000	3
Q345A	230×1597×10500	1
Q235A	230×1550×10800	8
Q235B	230×1550×9950	14
SAE1008	230×1600×9950	22
SPHC	230×1550×10800	5
08AL	230×1550×10800	4
RCL380	230×1550×10800	6

such as Hyper Mesh, ANSYS, and ANSYS Workbench [11,12,13]. Here, Hyper Mesh and ANSYS are adopted to analyze the main drive shaft of the rolling mill under dangerous working conditions.

FEM software ANSYS is an excellent numerical analysis and calculation software. In the field of linear computing, the position of ANSYS is quite stable [14]. ANSYS is a multi-physics field analysis package that integrates structure, fluid, electromagnetism and acoustics. Its common applications include industrial manufacturing, nuclear industry, household appliances, aerospace, and biomedicine. It has the most users in the world and is also a very successful FEM software [15].

Hyper Mesh software is a general FEM analysis software developed by Altair. It can be applied in the fields of modeling, visualization, automation and manufacturing, and is recognized and applied by the world industry. The shape of the drive shaft and bearing seat in the main drive device of the rolling mill is not too regular. Rough grids have low credibility and are likely to lead to incorrect calculation results. Since the quality of finite element mesh will directly affect the accuracy of final calculation results, finite element mesh is the key to analysis and calculation. The mesh quality greatly impacts the calculation results, and Hyper Mesh has the characteristics of a high-quality mesh division. It has a complete interactive two-dimensional and 3D cell division tool [16]. The user can adjust the mesh parameters of each face during the division process, such as cell density, cell offset gradient and mesh division algorithm. The 3D cell generation method provided by Hyper Mesh is employed to build high-quality tetrahedral and hexahedral meshes and Computational Fluid Dynamics meshes [17].

2. FEM model creation

The R2 rolling mill used in this section has a motor power of 7500kw and a motor speed of 45∼90rmp. According to the calculation equation, the maximum torque output at the motor end of the mill drive shaft is $1591000\mathrm{N}\cdot\mathrm{m}$. According to the functional relationship and parameters between the balance force on the drive shaft of the rolling mill and the driving force of the hydraulic cylinder, it is calculated that the balance force provided by the bearing seat is 348520N under the dangerous angle of the upper drive shaft of the rolling mill. The balance force provided by the bearing seat of the lower drive shaft of the rolling mill at a dangerous angle is 350100N. The material of the drive shaft in the main drive device of the rolling mill is 42Cr Mo. According to the manual, the elastic modulus of the drive shaft material in the main drive device of the rolling mill is 2.06×1011Pa, Poisson's ratio is 0.3, the maximum tensile strength of the material is 1080MPa, and the yield limit of the material is 930MPa. Other properties of materials can be calculated by empirical equation, such as torsion fatigue limit 301.5MPa, and fatigue limit 542.7MPa.

According to the calculated dangerous working condition angle of the rolling mill drive shaft, in the 3D software Solid Works, the drive shaft and bearing seat are virtually assembled. Then, it is saved to the file in .iges format to facilitate the reading of FEM software Hyper Mesh.

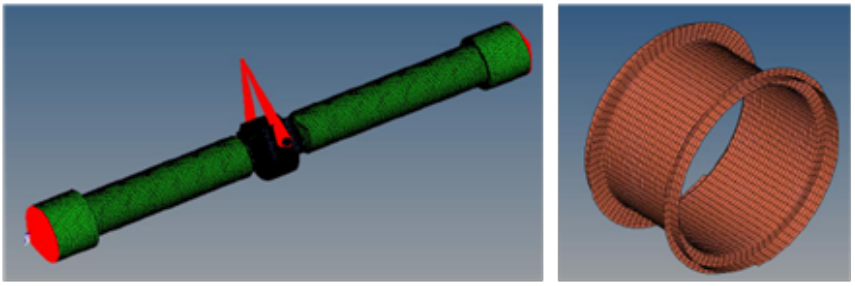

Fig. 2.3: Mesh element model and contact element (a) Mesh element model; (b) Contact element

FEM software Hyper Mesh is started. Because the solution and calculation phase need to be carried out in ANSYS, the ANSYS panel is selected in the Load User Profile. When importing a model, the i MPortgeometry option is selected to import the .iges format file previously saved through Solid Works into Hyper Mesh. The mesh of the rolling mill's imported main drive shaft and the bearing seat model are divided. In order to make the divided element mesh neat and regular, the area where the balance force is added in the bearing seat is coupled with the bearing seat by establishing a contact surface, as shown in Figure 3(a). The cell type selected is SOLID185 cell. There is contact between the drive shaft and the bearing seat, so it is essential to establish contact between the bearing and the drive shaft, as shown in Figure 3(b). The contact pairs are CONTA173 and TARGE170.

Then, the dangerous angle of the upper drive shaft and the lower drive shaft of the rolling mill can be judged according to the theoretical calculation results. Then, through rotation in Hyper Mesh, the data file of dangerous working conditions of the main drive shaft of the rolling mill is obtained. In order to add the constraints of the two dangerous angles of the main drive shaft of the rolling mill correctly, it is necessary to establish a local coordinate system at both ends of the drive shaft. The number of the local coordinate system at the motor end and at the roll section is set to 20 and 21, respectively, to prevent errors in the simulation. The constraint added at the motor end is to limit the three degrees of freedom of displacement of the motor end face. The constraint added at the roller end is to limit the three degrees of freedom of displacement of the roller end and the degrees of freedom of rotation in the Z-axis direction (axial direction).

3. Static strength simulation analysis
   After the preprocessing of Hyper Mesh, it is essential to open the saved data file in ANSYS and solve it. After the solution is completed, the stress change nephogram of the main drive shaft of the rolling mill can be obtained under the dangerous working angle of the drive shaft in the main drive device of the rolling mill. The material selected is 42Cr Mo, which is plastic material. The fourth strength theory (Von Mises) is used as the criterion for strength judgment. It is believed that the density of distortion energy or the specific energy of shape change is the main reason for material yield failure. Von Mises Stress is output in the post-processing [18].

(2) Fatigue strength check of the main drive shaft of the R2 rolling mill. First, the final element calculation of the drive shaft at a dangerous angle is conducted to determine whether the design strength of the drive shaft meets the requirements. Then, through the analysis of the working state of the drive shaft, the bending moment of the drive shaft of the rolling mill is the alternating stress. As the rolling mill is reversible, the torque of the drive shaft is also alternating stress. The fatigue strength of the drive shaft at the dangerous angle of the mill drive shaft is checked.

According to the fatigue limit σ_{-1} of the material under symmetrical cyclic alternating stress, the fatigue

limit $(\sigma_{-1})_G$ and allowable stress $[\sigma_{-1}]$ of the drive shaft can be calculated. Their values are:

$$(\sigma_{-1})_G = \frac{\varepsilon_\sigma \beta}{K_\sigma}\sigma_{-1} \tag{2.1}$$

$$[\sigma_{-1}] = \frac{(\sigma_{-1})_G}{n} \tag{2.2}$$

n represents the allowable safety factor. Generally, according to the regulations, when the material quality is uniform and the calculation accuracy is high, n=1.3∼1.5. According to the engineering calculation, the allowable safety factor is 1.5. ε_σ is the size factor of the component, with a value of 0.53. is the surface processing coefficient, and the value is 1.

When the rolling mill is at a dangerous working angle, the bending moment of sections A-A and B-B are calculated. Since the direction of gravity is not perpendicular to the axis direction, the gravity component perpendicular to the axis direction is adopted to calculate the bending moments of the transmission shaft sections A-A and B-B when calculating the bending moments of the above sections. Finally, according to the theoretical data, the maximum working stress of the rolling mill drive shaft at the dangerous section A-A and B-B can be calculated.

In order to calculate the safety factor closer to the real situation, the maximum working stress and maximum shear stress of the dangerous section are extracted from the post-processing of ANSYS. The post-processing interface of ANSYS is opened. In the command flow window of ANSYS, RSYS,20 are input to make the stress distribution of the drive shaft along the axial direction. It is convenient to extract the stress distribution diagram of the rolling mill drive shaft in the dangerous area to complete the fatigue strength check of the rolling mill drive shaft.

3. Simulation experimental results.

3.1. Test results of mechanical mechanics parameters of main drive electromechanical coupling system of R2 rolling mill .

(1) Distribution probability of peak and average rolling force. Figure 3.1 presents the distribution probability results of the peak and average rolling force of the electromechanical coupling system of the main drive of the R2 rolling mill.

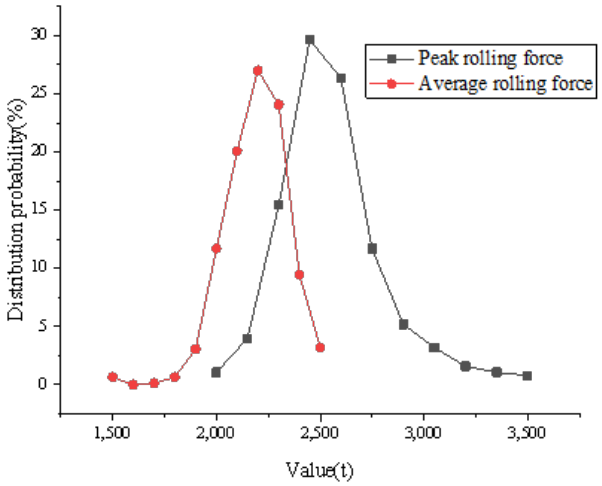

Fig. 3.1: Distribution probability diagram of peak and average rolling force

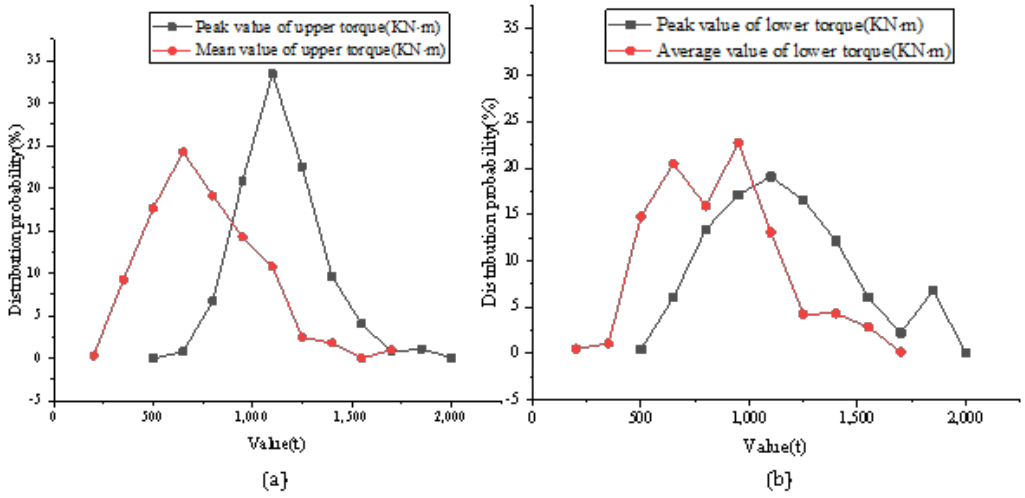

Fig. 3.2: Distribution probability of torque peak value and average value (a) Distribution probability of peak value and the average value of upper torque; (b) Distribution probability of the peak and the average value of the lower torque

Figure 3.1 reveals that the measured average value of rolling force is in the range of 1230∼2660t, and the peak value is in the range of 1400∼3620t. The results of the probability distribution of the peak rolling force show that the peak rolling force is mainly distributed in the range of 2300∼2750t. The average distribution probability of rolling force suggests that the average distribution of rolling force is mainly in the range of 2000∼2400t.

(2) Distribution probability of torque peak and average. Figure 3.2 displays the probability results of the peak and average distribution of the upper torque and lower torque of the electromechanical coupling system of the main drive of the R2 rolling mill.

Figure 3.2 illustrates that the peak value of the upper torque is mainly distributed in the range of 800∼1400

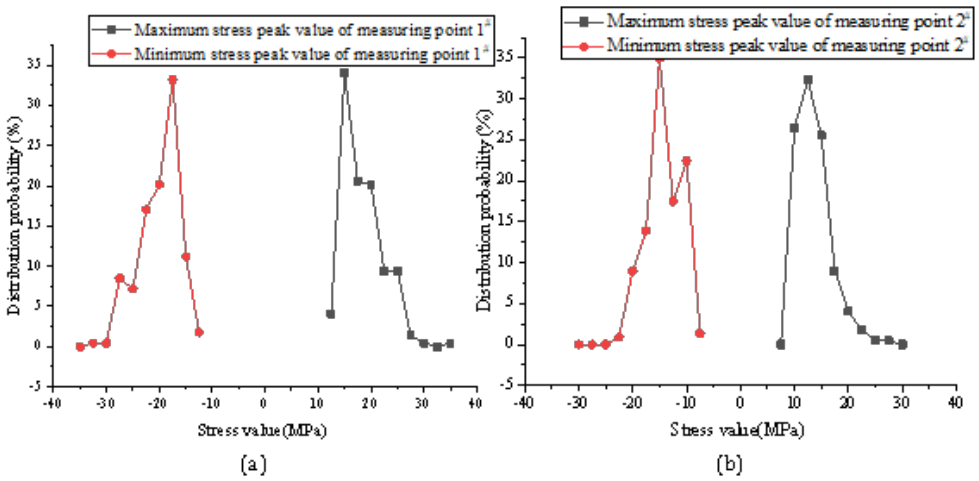

Fig. 3.3: Distribution probability of stress peak at different measuring points (a) Distribution probability of stress peak at measuring point $1^{\#}$; (b) Probability of stress peak distribution at measuring point $2^{\#}$

mk N, and the average value of the upper torque is mainly distributed in the range of 350∼1100 mk N. The peak value of the lower torque is mainly distributed in the range of 650∼1550 mk N, and the average value of the lower torque is mainly distributed in the range of 500∼1100 mk N.

(3) Distribution probability of stress peak. The fatigue of metal structure is closely related to the main cycle characteristics of structural stress, and the small fluctuation of stress has little effect on fatigue life. Hence, the change of stress amplitude at each measuring point during the rolling process is recorded, and the stress equivalent curve of each measuring point is made.

Figure 3.3 displays the distribution probability of the maximum principal stress peak at different measuring points (near the drive side) after testing.

Figure 3.3 suggests that the maximum principal stress peak value of $1^{\#}$ measuring point is within the range of 10-35Mpa, and the minimum principal stress peak value of $1^{\#}$ measuring point is within the range of 10-30Mpa. The maximum principal stress average value is 24Mpa, and the minimum principal stress average value is -24Mpa. The maximum principal stress peak value of $2^{\#}$ measuring point is in the range of 5-25Mpa, the minimum principal stress peak value of $2^{\#}$ measuring point is in the range of 8-22Mpa, the maximum principal stress average value is 16Mpa, and the minimum principal stress average value is -16Mpa. During idling, the maximum and minimum principal stress values of $1^{\#}$ and $2^{\#}$ measuring points are 8Mpa.

(4) Torsional vibration power change of main drive system of R2 rolling mill. The first natural frequency of the upper and lower main drive systems can be obtained by power spectrum analysis of the measured torsional vibration waveforms of the upper and lower main drive systems, as shown in Figure 3.4.

Figure 3.4 suggests that the torsional vibration power spectrum of the upper and lower main drive systems of the R2 rolling mill is basically similar, and both reach a peak at about 17.5Hz.

3.2. Strength simulation analysis results of the main drive shaft of the R2 rolling mill. Figure 3.5 presents the stress distribution nephogram of the drive shaft of the rolling mill when the upper drive shaft is at different working angles.

Figure 3.5 suggests that when the upper drive shaft of the rolling mill is at a working angle of 1.02°, the maximum Von Mises Stress of the drive shaft of the rolling mill is 95.10MPa. It appears in the transition shaft shoulder's fillet area where the main drive shaft of the rolling mill contacts the bearing seat. When the lower drive shaft of the rolling mill is at a working angle of 3.14°, the maximum Von Mises Stress of the rolling mill drive shaft is 95.15MPa. It appears in the transition shaft shoulder's fillet area where the main drive shaft of the rolling mill contacts the bearing seat. The analysis reveals that the Von Mises Stress value of the rolling mill drive shaft is far less than the yield limit of 930MPa.

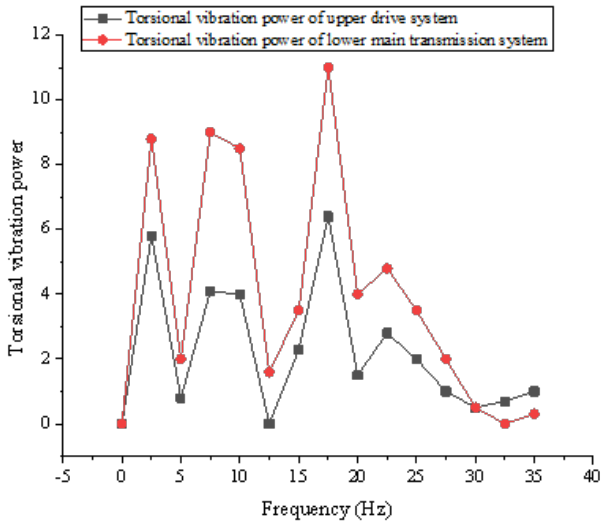

Fig. 3.4: Torsional vibration power spectrum of upper and lower main drive systems of R2 rolling mill

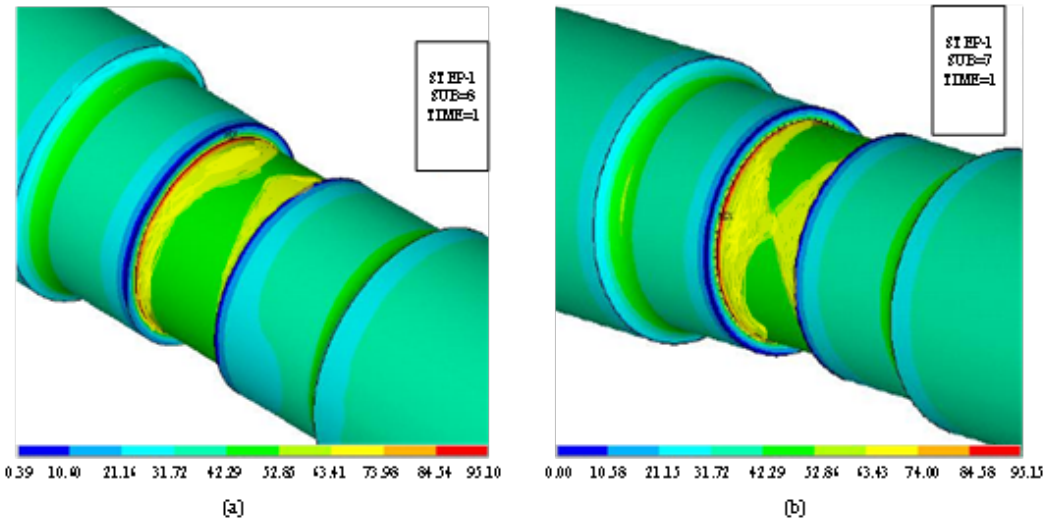

Fig. 3.5: Stress distribution nephogram of rolling mill drive shaft under different working angles (a) Stress distribution nephogram of rolling mill drive shaft at 1.02° working angle; (b) Stress distribution nephogram of the lower drive shaft in the main drive device of the rolling mill at a working angle of 3.14°

4. Conclusion. This work further analyzes and tests the compressive strength of the electromechanical system of the main drive coupling of the R2 rolling mill through testing and simulation experiments based on previous scholars' research on the electromechanical system of the main drive coupling of the rolling mill. Besides, the strength of the main drive shaft in the main drive coupling electromechanical system of the R2 rolling mill is analyzed. The research results show that the peak value of the lower torque of the main drive coupling electromechanical of the R2 rolling mill is mainly distributed in the range of 650∼1550 mk N, and the average value of the upper torque is mainly distributed in the range of 350∼1100 mk N. When the upper drive shaft of the rolling mill runs at a working angle of 1.02°, the maximum Von Mises Stress of the drive shaft of

the rolling mill is 95.10MPa. When the drive shaft of the rolling mill operates at a working angle of 3.14°, the maximum Von Mises Stress of the drive shaft of the rolling mill is 95.15MPa. The research deficiency is that only the whole part of the main drive coupling electromechanical system of the R2 rolling mill and the strength of the rotating shaft have been studied, while the strength of other structures has not been studied. Later, it will be studied and analyzed to provide some reference for improving the strength of the main drive coupling electromechanical system of the rolling mill.

REFERENCES

[1] Sanjari R. K. S. S. (2021) Semi-quantitative health risk assessment of exposure to chemicals in an aluminum rolling mill[J]. International Journal of Occupational Safety and Ergonomics, 27(2), 22-23.
[2] Ramirez-Tamayo D., Soulami A., Gupta V., et al. (2021) A complex-variable cohesive finite element subroutine to enable efficient determination of interfacial cohesive material parameters[J]. Engineering Fracture Mechanics, 247(14), 107638.
[3] Nazaretov A. A., Yaitskov I. A., Chukarin A. N. (2021) The Derivation of the Noise Level Dependences and Vibration Velocities of Elements and Units of the Drive System of the Rail Grinding Machines[J]. IOP Conference Series: Earth and Environmental Science, 720(1), 012014.
[4] Zhang Z., Ji W., Yang B., et al. (2022) Dynamic analysis and vibration reduction of mechanical-hydraulic coupled tunnel boring machine (TBM) main drive system:[J]. Proceedings of the Institution of Mechanical Engineers, Part C: Journal of Mechanical Engineering Science, 236(1), 115-125.
[5] Zhang G., Bao J., Li W., et al. (2021) Coupled Vibration Characteristics Analysis of Hot Rolling Mill with Structural Gap[J]. Shock and Vibration, 2021(3), 1-10.
[6] Liu Z., Zhang X., Zhu Z., et al. (2021) Study on Dynamic Amplification Factor of UHV Pillar Equipment[J]. IOP Conference Series Earth and Environmental Science, 791(1), 012141.
[7] Thomas G., Campbell O., Nichols N., et al. (2021) Formulating and Deploying Strength Amplification Controllers for Lower-Body Walking Exoskeletons. [J]. Frontiers in robotics and AI, 8(3), 720231.
[8] Wang Q. H., Liu X., Wang D. N. (2021) Ultra-sensitive gas pressure sensor based on vernier effect with controllable amplification factor[J]. Optical Fiber Technology, 61(13), 102404.
[9] Fanaie N., Nadalipour Z., Sarkhosh O. S., et al. (2021) Elastic drift amplification factor in steel moment frames with double reduced beam section (DRBS) connections[J]. Journal of Building Engineering, 43(43), 1-22.
[10] Rsel G. (2021) Strength-based design of a fertilizer spreader chassis using computer aided engineering and experimental validation[J]. Proceedings of the Institution of Mechanical Engineers, Part C: Journal of Mechanical Engineering Science, 235(12), 095440622199384.
[11] Tai J., Li H., Guan Y., et al. (2021) Simulation of a maize ear picking device with a longitudinal horizontal roller based on hypermesh modeling[J]. Bioresources, 16(1), 1394-1410.
[12] Lin Y., Xie X., Yan L., et al. (2022) Research on the collapse of Tacoma narrows bridge under the finite element application ANSYS of computational mechanics[J]. Journal of Physics: Conference Series, 2230(1), 012018.
[13] Li J., Pan M., Sun K., et al. (2022) Mechanical Characteristics Analysis of Grinding Plate of Food Waste Grinding Mill Based on ANSYS Workbench[J]. Journal of Physics: Conference Series, 2152(1), 012021.
[14] Adhikari N., Alexeenko A. (2021) Development and Verification of Nonequilibrium Reacting Airflow Modeling in ANSYS Fluent[J]. Journal of Thermophysics and Heat Transfer, 2021(1):1-11.
[15] Khan N. B., Ibrahim Z. B., Ali M. A., et al. (2021) Numerical simulation of flow with large eddy simulation at Re = 3900[J]. International Journal of Numerical Methods for Heat & Fluid Flow, 30(5), 2397-2409.
[16] Wang M., Dong M., Lu S., et al. (2021) Modal analysis of excavator toolbox based on hypermesh[J]. Journal of Physics Conference Series, 1965(1), 012037.
[17] Zhang T. (2021) Lightweight Analysis Based on the Hypermesh Frame[J]. Mechanical Engineering and Technology, 10(3), 407-418.
[18] Ji D., Hu X., Zhao Z., et al. (2022) Stress Rupture Life Prediction Method for Notched Specimens Based on Minimum Average Von Mises Equivalent Stress[J]. Metals, 12(1), 68.

Edited by: B. Nagaraj M.E
Special issue on: Deep Learning-Based Advanced Research Trends in Scalable Computing
Received: Dec 28, 2023
Accepted: Mar 20, 2024